Electronic Control of Chemistry and Catalysis at the Surface of an Individual Tin Oxide Nanowire

ARTICLE *in* THE JOURNAL OF PHYSICAL CHEMISTRY B · MARCH 2005

Impact Factor: 3.3 · DOI: 10.1021/jp045509l · Source: PubMed

Electronic Control of Chemistry and Catalysis at the Surface of an Individual Tin Oxide Nanowire

Y. Zhang, A. Kolmakov,* Y. Lilach, and M. Moskovits*

Department of Chemistry and Biochemistry, University of California−Santa Barbara, Santa Barbara, California 93103-9510

Received: October 2, 2004; In Final Form: November 26, 2004

Tin oxide single nanowires configured as field effect transistors were shown to be operable and tunable alternately as gas sensors or as catalysts under a gaseous atmosphere that simulated realistic ambient conditions. The unusually large surface-to-volume ratio available with nanowires causes adsorption or desorption of donor or acceptor molecules on the nanowire's surface to greatly alter its bulk electron density at relatively small values of the gate voltage. This process can be sensitively monitored as changes in the nanowire's conductivity. The potentially radical change in carrier density can lead to significant changes in the nanowire's sensitivity as a sensor or reciprocally as a catalyst in reactions that involve charge exchange across the nanowire's surface. This leads to the prospect of tuning catalysis or other surface reactions entirely through electronic means.

1. Introduction

Metal oxide nanowires are poised to impact on such varied technologies as electronics and optoelectronics, lasers, solar energy conversion, environmental sensing, and catalysis.[1−6] Their large surface-to-volume ratio and their function as quasi-one-dimensional conductive elements simultaneously confer upon them high sensitivity and size-dependent transduction of the chemical processes occurring at their surface into functional electrical signals. Significant progress has already been reported involving carbon nanotubes and semiconductor nanowires[7−10] as sensors and in other electronic applications. Contrariwise, the fabrication of devices based on metal oxide nanowires is still largely undeveloped[3,4,11,12] despite the fact that metal oxides are widely used as support materials for catalysts and as gas sensors.[13−17] In this paper, which builds on a previous report,[18] we report the successful fabrication of a three-terminal source−gate−drain single-nanowire field effect transistor (FET) device based on template-synthesized as well as vapor-grown SnO_2 nanowires and explore the electron-transport properties of these nanowire devices as a function of temperature, gas environment, and gate potential. We find that chemisorption of oxygen as well as interactions with gases such as CO can greatly change the electron density inside the nanowire. Reciprocally, oxygen adsorptivity can be completely shut down, and as a result, the subsequent catalytic conversion of CO to CO_2 at the SnO_2 surface can be dramatically altered upon modulating the electronic state of the material by applying an appropriate gate potential. By close analogy to processes taking place in macroscopic metal oxide semiconductor field effect transistor (MOSFET) gas sensors,[19,20] this observation immediately brings to mind gate-tunable nanowire-based FET gas sensors wherein the gate potential metaphorically plays a role not unlike changing the surface functionality of the sensor. Likewise, the observation implies the possibility of gate-tunable catalysts whose species-selective reactivity, sensitivity, and response time can be electronically controlled.

2. Experimental Section

The nanowires used in this study were prepared using two different synthetic methods. In the first, arrays of parallel tin nanowires with predefined, dimensionally uniform diameters and lengths were electrochemically synthesized inside the pores of highly ordered porous anodic alumina (PAO) templates as previously described.[21−25] Highly crystalline, metallic β-Sn nanowires (60 nm average diameter and average length determined by the template thickness of $\sim$50 μm in this study) were electrochemically grown in pores of the templates and subsequently removed from their matrix, suspended in a solvent, diluted, and deposited on a p-Si (boron-doped 0.02 Ω cm) substrate covered with a 300 nm thermally grown SiO_2 film. Individual Sn nanowires were topotactically oxidized to SnO_2 by annealing in air over several hours at several gradually increasing temperature steps eventually reaching 823 K.[26] Transmission electron microscopy (TEM) and X-ray diffraction (XRD) analysis confirmed the nanowire integrity after oxidation and its complete oxidation to (rutile) polycrystalline SnO_2 with crystalline domains ($\sim 10^2-10^3$ nm) greatly exceeding the nanowire's diameter. Higher-crystallinity nanowires were grown from the vapor phase using so-called vapor−solid synthesis.[2,27] Briefly, single-crystal SnO_2 nanowires and nanobelts were grown by chemical vapor deposition of SnO in a tube furnace at 1000 °C in an Ar carrier gas (50 sccm, 200 Torr) containing traces of oxygen. The structure, stoichiometry, and morphology of the resultant one-dimensional (1-D) nanostructures were verified with scanning electron microscopy (SEM), high-resolution TEM, Raman spectroscopy, and XRD, which agree well with previous reports.[2,11,27] Conductance measurements were carried out on isolated individual nanowires as a function of the gas composition and temperature in a custom-designed 100 mL gas cell. Electrical contacts to the nanowire were vapor deposited Ti (20 nm)/Au (200 nm) micropads, which acted as the source and drain electrodes. The Si substrate was used as

* Corresponding authors. E-mail: akolmakov@physics.siu.edu; mmoskovits@LTSC.ucsb.edu.

10.1021/jp045509l CCC: $30.25
Published on Web 01/15/2005

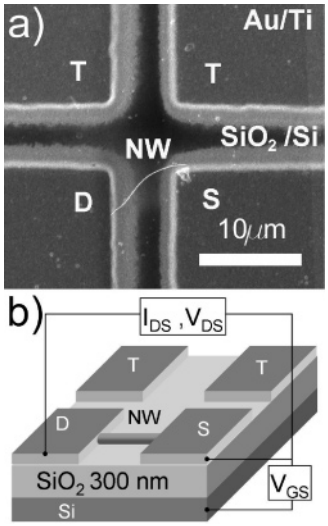

Figure 1. (a) SEM image of a SnO_2 nanowire deposited on a SiO_2 substrate outfitted with Au/Ti electrodes. (b) Schematic of the nanowire FET. The Si support also functions as the gate electrode G, S, D, and T are, respectively, the source, drain, and a pair of reference electrodes unconnected by a nanowire.

the back-gate electrode (Figure 1). Conductance changes resulting from chemical processes at the surface of the SiO_2 substrate as well as the source−drain and source−gate leakage currents were determined using a pair of neighboring reference electrodes (electrodes "T" in Figure 1) that were not connected by a nanowire. In the absence of oxygen and water vapor, the leakage currents were below 3 nA at the maximum voltage (10 V) and the highest temperature (620 K) used in these experiments. The electron-transport properties of some 20 single-crystal and polycrystalline individual tin oxide nanowires fabricated in several separate runs and using the two synthesis methods referred to above were measured. Mindful of the fact that nanowires of various diameters and lengths were used, all of the measurements gave very similar qualitative results, indicating that the observed behavior was a robust property of the nanowires and the devices fabricated from them. However, the quantitative measured values of the conductivity, electron mobility, activation energies, etc. showed some variation depending on the quality of the metal-to-nanowire contact and the nanowire's pretreatment history and especially on the estimated stoichiometry of the oxide, the relative humidity of the ambient, and the age of the nanowire. In addition, time-dependent and hysteresis effects were sometimes observed in $I_{DS}(V_{DS,GS})$ measurements. The latter effect is believed to be due to the finite accumulation and relaxation times of field-induced charges localized at traps at the various oxide interfaces.[28] To minimize these influences and establish a reference steady-state condition, the results presented here were obtained from nanowires that were pretreated at 550−580 K under flowing dry N_2 for 2 h at the gate potential for which the experiments were conducted.

3. Results and Discussion

3.1. Electronic Properties of Nanowires under Inert and Oxidizing Environments. Most of the SnO_2 nanowires studied showed significant conductance sensitivity toward oxidizing and reducing gases (Figure 2a) and a prominent gate effect (Figure 2b) as an n-channel (normally on) FET. A few operated as normally off FETs, exhibiting a positive shift of the threshold voltage probably resulting from residual surface charge at the SiO_2 surface or silicon/SiO_2 interface near the nanowire. Because

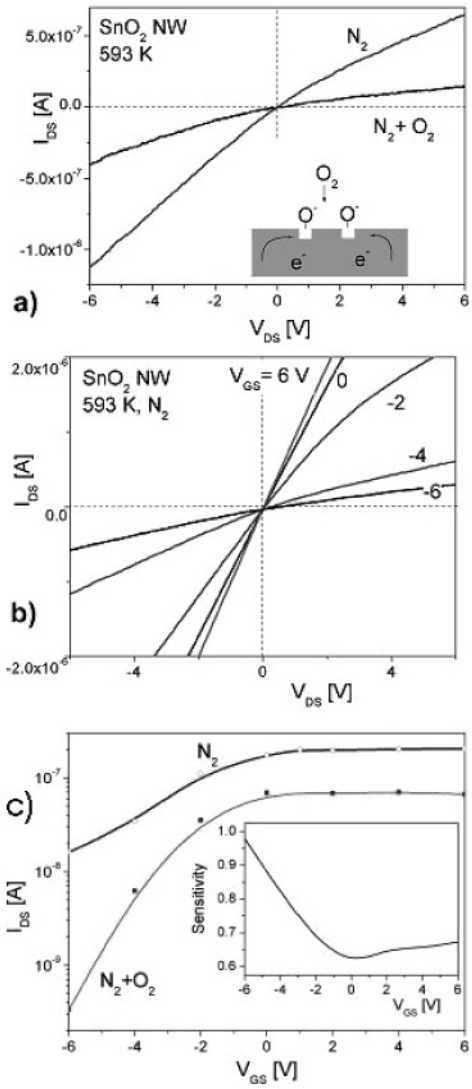

Figure 2. (a) Current−voltage characteristics, I_{DS} (V_{DS}), at $V_{GS} = 0$ V for a 60 nm SnO_2 nanowire as a function of the composition of (flowing) ambient gas at 573 K. Top: 100 sccm flow of dry N_2. Bottom: with added 10 sccm of O_2. (b) As in part a, but for various values of the gate voltage. (c) I_{DS} (V_{DS}) measured in different gas environments. (V_{DS} = 200 mV, all other parameters as in part a). Inset: the nanowire's sensitivity, $Y = (G_{N_2} - G_{O_2})/G_{N_2}$ toward 10 sccm of O_2 as a function of gate voltage.

of the large surface-to-bulk ratio and the fact that the characteristic nanowire's radius (∼20−50 nm) is comparable or less than the Debye length for SnO_2 in the temperature range used,[29] one can expect the nanowire's electronic and transport properties (and therefore its FET performance) to be strongly, indeed primarily, affected by surface processes, as observed. The measured source−drain (I_{DS}) current and transfer characteristics of NW FET were found to depend critically on the composition of ambient gas (Figure 2) and temperature.[30] Under dry nitrogen (and after several hours' annealing) the nanowire becomes a fairly good conductor, whose conductivity ($\sigma_{V_G=0}$ = 220 (Ω cm)$^{-1}$ at 300 C°) depends only moderately on gate potential (top curve in Figure 2c). In many cases, the switching ratio under these conditions was only 5−10 with the gate field being unable to affect the current appreciably. In the presence of oxygen, the nanowire's conductivity drops significantly ($\sigma_{V_{GS}=0}$ = 74 (Ω cm)$^{-1}$), and an enhanced gate effect with a much higher switching ratio (Figure 2, bottom curve) is observed. The highest switching ratios (∼10^3) were observed in air at room temperature

for vapor-grown SnO_2 nanowires. Although large, this value is lower than a record value of 10^4 reported for nanobelts.[4] As was previously reported for metal oxide nanowire and nanobelt FETs,[4,12] the adsorption of acceptor molecules on the surface of the nanowire causes a positive shift in the threshold voltage, indicating a reduction in the electron density. By use of the nanowire's gate capacitance $C \cong 2\pi\epsilon\epsilon_0 L/\ln(2h/R)$ (where L and R are the length and radius of the nanowire and h and ϵ are the thickness and dielectric constant of the gate oxide) and the measured threshold voltage V_{th}, the electron density ($n = CV_{th}/e\pi R^2 L$) is determined to be $\sim 10^{18}$ cm^{-3} in air at 573 K as compared to $\sim 10^{19}$ cm^{-3} when the nanowire is under dry nitrogen (assuming the conductance drop upon exposure to oxygen to be entirely due to a change in electron density). These values are within an order of magnitude of those reported for the single-crystal tin oxide[29] under similar ambient conditions.

The electronic properties of the bulk and the surface of SnO_2 are well documented[31,32] and therefore provide a basis for understanding electron exchange between surface acceptor states and bulk states of the metal oxide nanowire, noting that for SnO_2 the Debye length at temperatures 300−600 K lies in the range 200−30 nm, respectively,[29] comparable to or larger than the nanowire's radius. Consequently, flat-band conditions apply to the nanowire in the radial direction, implying essentially no barriers to electron transfer at the nanowire's surface. As previously reported,[29] under flat-band conditions, charge conservation in a long, thin, cylindrical wire simplifies to the expression

$$N_s\theta = \frac{R}{2}(n_0 - n_m) \qquad (1)$$

where N_s is the surface density of adsorption sites (cm^{-2}), θ is the fraction of nanowire surface covered with adsorbate ($\theta_{max} = 1$), and n_m is the density of itinerant electrons remaining in the nanowire after exposure to the adsorbate.

For SnO_2 at $\sim$600 K and at zero gate potential, the material's high conductance $G(N_2) = \pi R^2 e\mu n_0/L$ in the absence of oxygen (i.e., when $n_0 = n_m$, Figure 2a) results from the presence of shallow donor states consisting of a high density of oxygen vacancies

$$V_0 \overset{kT}{\longleftrightarrow} V_0^{\gamma+} + \gamma e^-$$

which can be totally ($\gamma = 2$) or partially ($\gamma = 1$) ionized. The latter also renders the oxide an n-type semiconductor. Under these conditions, the Fermi level is just below the conduction band edge. The resulting high carrier density also accounts for the negative shift of the threshold voltage, the FET's large "off" state current (Figure 2, parts b and c, top curves), and the small temperature coefficient of the conductance as reported previously.[30]

Exposure to oxygen saturates the surface vacancies, drawing electrons from the bulk and localizing them on the ionically adsorbed (ionosorbed) oxygens (Supporting Information). In contrast to large-diameter ($D \gg \lambda_D$) wires, where oxygen chemisorption induces band bending near the wire's surface, the effect of adsorption on small-diameter nanowires is to change the location of the Fermi level within the band gap of the nanowire. The accompanying electron depletion $\Delta n = 2N_s\theta/R$ results in a significant drop in conductance

$$G(O_2) = \frac{\pi R^2 e\mu}{L}\left(n_0 - \frac{2N_s\theta}{R}\right) \qquad (2)$$

(Figure 2a, bottom curve) and a corresponding increase in activation energy.[30] (We neglect the dependence of the mobility on the surface coverage, a reasonable approximation when the electron diffusion length ($\sim$1 nm) is much smaller than the nanowire's diameter ($\sim$60 nm), which is the case at the temperature used.[29]) The reduced electron density also magnifies the effect of the gate potential, resulting in the efficient switching of the source−drain current (I_{DS}) and a positive shift of the threshold value in the FET's transfer function (Figure 2) when the back-gate electrode potential, V_{GS}, becomes sufficiently negative. This effect, typical for an FET based on an n-doped semiconductor, was previously observed in other nanowire-based FETs,[33−38] including the recent results on SnO_2 nanobelts.[4] On the basis of this observation, the sensitivity, $Y = (G_{N_2} - G_{O_2})/G_{N_2}$, of the nanowire configured as an FET and operating as an oxygen sensor (insert in Figure 2) can also be maximized by tuning the gate potential to the threshold voltage appropriate to the specific gas environment being probed.

3.2. Influence of Gate Potential on Sensing and on the Catalytic Performance of the Nanowire. For reactions involving ionosorbed oxygen (i.e., an oxygen species that is ionized by charge transfer during chemisorption, under our conditions resulting largely[29] in O^-) as a reactant, such as the catalytic oxidation of CO, one would also expect the extent, rate, and selectivity of the catalytic reactions occurring on the nanowire's surface to be gate−voltage controllable. To better understand the interplay between adsorption, electron transport, catalysis, and gate voltage on the FET-configured SnO_2 nanowire, the variation of I_{DS} at $V_{DS} = 1$ V as a function of the partial pressures of nitrogen, oxygen, and CO were measured at various values of the gate potential (Figure 3a). The baseline I_{DS} is taken to be its steady-state value, measured following prolonged exposure to dry N_2 at each of the gate-potential values and temperatures used. In contrast to the FET transfer characteristics shown in Figure 2c, which were carried out immediately after changing the value of V_{GS}, the following measurements were carried out after sufficient time was allowed to lapse ($\sim$2 h) so as to allow the system to reestablish a new electronic and thermodynamic steady state. At time t_1, 10 sccm of oxygen gas was mixed into the 100 sccm nitrogen flow. This was followed at time t_2 by the addition of CO (5 sccm) into the gas flowing into the cell. A few important observations can be deduced from Figure 3a. The steady-state value of the conductance in dry nitrogen G_{N_2} decreases monotonically when the gate potential is made more negative, dropping $\sim$70-fold when V_{GS} is reduced to approximately −6 V. When the gate potential is made progressively more positive, the conductance increases, then achieves an approximately constant value. The conductance decreases greatly when oxygen is introduced. However, the size of this decreasing ΔG_{O_2} diminishes with decreasing (and negative) gate potential until at $V_{GS} \approx -6$ V and below this oxygen-induced conductance drop essentially vanishes. Assuming the conductance decrease to be proportional to the coverage of ionosorbed oxygen, a zero value of ΔG_{O_2} (Figure 3, part a, bottom, and part b) implies that ionosorption no longer takes place. (Of course, one cannot be sure that physisorbed oxygen is absent from the surface.) Almost immediately upon the introduction of CO, the conductance increases, eventually achieving a new steady state. We associate this conductance increase with the catalytic oxidation of CO, which alters the steady-state coverage of ionosorbed oxygen. In contrast with what was observed on introducing oxygen only, the observed conductance increase on admitting CO is not monotonic with the gate voltage but achieves a maximum value in the range

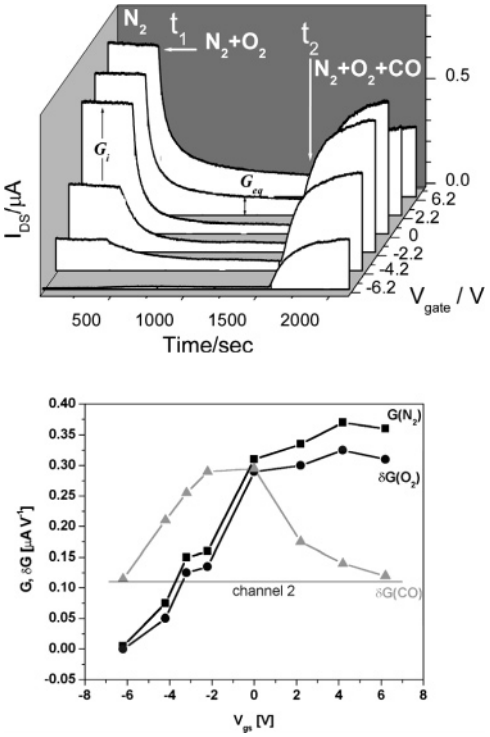

Figure 3. (a) The response of the nanowire's source−drain current (V_{DS} = 2 V) to the addition of 10 sccm of oxygen to 100 sccm of flowing nitrogen gas at time t_1 followed by the addition of 5 sccm of CO at time t_2 at various values of the gate potentials at 553 K. (b) The extent of reaction with oxygen, ΔG_{O_2}, and CO, ΔG_{CO}, as a function of gate voltage assumed to be proportional to the values of the conductance decrease (increase) (part a) when O_2 (CO) gas is sequentially admitted into the gas cell. The nanowire conductance under dry nitrogen, G_{N_2}, is included for comparison. Also shown, the extent of reaction of CO through a putative second reaction channel that does not involve ionosorbed oxygens as a reagent.

V_{GS} = −2 to 0 V for this particular FET. Interestingly, even at V_{GS} = −6 V, when oxygen ionosorption no longer takes place, the introduction of CO causes the conductance to increase. We can adequately account for the observed response of the conductance to gate voltage and ambient gas composition using an empirical two-state kinetic model, which is outlined below. In the following section, we consider the descending and rising parts of the conductance response separately to elucidate the processes accompanying the adsorption−desorption kinetics in the two gaseous environments (N_2/O_2 and N_2/O_2/CO).

3.2.1. Oxygen Ionosorption. Equation 2 indicates that the conductance change, ΔG_{O_2}, (deduced from the change in the value of I_{DS} as measured in a pure nitrogen atmosphere and that measured after oxygen gas was mixed into the flowing nitrogen) can be used as a quantitative measure of the ionosorbed oxygen surface coverage. The quantity ΔG_{O_2} is determined by fitting an empirical biexponetial curve to the measured kinetics then using the parameters extracted to determine the initial and final values of the conductance (Supporting Information). (A similar value, ΔG_{CO}, is defined for the rising portion of the conductance curve observed when CO was also added to the flowing gas. Moreover, both quantities were determined from the "first cycle", that is, the first time the oxygen and CO were turned on after the nanowire was exposed for 2 h to flowing dry nitrogen.) Figure 3b shows a plot of ΔG_{O_2} and ΔG_{CO} as a function of gate voltage. Measured values of $G(N_2)$, the source−drain current measured with the system under nitrogen *before* the oxygen flow is begun, are also included in Figure 3b. ΔG_{O_2} and $G(N_2)$ are found to have a very similar trend with gate voltage. Specifically, for negative values of the gate voltage, both functions decrease gradually with decreasing gate voltage and can be made to vanish at sufficiently negative values of the gate voltage. This behavior is immediately understandable using simple model introduced above. Negative values of the gate voltage decrease the electron density

$$n = \frac{C}{\pi R^2 L}(V_{GS} - V_{th}) \tag{3}$$

in the nanowire approximately linearly, decreasing its conductance $G(N_2)$. Likewise, because the repopulation of the oxygen defects (which we have heretofore assumed to be through ionic chemisorption of oxygen on the nanowire surface) makes use of and localizes electrons from the bulk of the nanowire onto the surface oxygens, as the electron concentration decreases so will the capacity for ionic chemisorption of oxygen. Combining eqs 1 and 3 produces an expression for the dependence of the oxygen coverage with gate potential

$$\theta = \frac{C\alpha}{2\pi RLN_s}(V_{GS} - V_{th}) \tag{4}$$

as approximately observed. In eq 4, the quantity $\alpha = 1 - n_m/n_0$ (assumed to be a gate-potential-independent parameter due to the proportionality between n_m and n_0) is the "electron capture efficiency", which presumably is responsible for the slight difference in slope between the gate dependence measured in the presence of ionosorption and the slope measured in a pure nitrogen environment. In fact, because the electrons can be regarded as a reagent in the ionosorption process and oxygen is in excess, the extent of oxygen chemisorption (ΔG_{O_2}) should track the carrier concentration closely, precisely as observed. Because the nanowire's surface-to-volume ratio is very large (there are only some 10^5 carriers in the nanowire), it is easy to attain fields strong enough (at low values of the gate voltage) to reduce the free carrier concentration essentially to zero, shutting down the oxygen chemisorption process and all subsequent surface processes in which ionically chemisorbed oxygen is a reactant.

For positive values of the gate voltage, both ΔG_{O_2} and $G(N_2)$ are found to increase slightly with increasing gate voltage, eventually reaching a plateau. The positive fields draw in excess electrons into empty states on the nanowire (Figure 2c), but ΔG_{O_2} and $G(N_2)$ saturate due both to the saturation of available states and to the nonzero contact resistance at nanowire leads. The latter effects limit free electron density in the nanowire and as a result saturate the adsorption capacity of the nanowire's surface.

3.2.2. CO Oxidation and Gate-Controlled Selectivity. The effect of varying the gate potential on the conductance increase when CO is mixed into the nitrogen/oxygen flow (at time t_2) is shown in Figures 3, parts a and b. In accordance with the accepted mechanism,[29] the increase of conductance is ascribed to the reduction in coverage of the ionosorbed oxygen consumed as a result of the catalytic oxidation of CO to CO_2 in one or more of the following processes[39]

$$CO^g + S \rightarrow CO^S \tag{5a}$$

$$CO^S + O_S^- \rightleftharpoons CO_{2,S}^- \rightleftharpoons CO_2^g + e^- \tag{5b}$$

$$CO^S + 2O_S^- \rightleftharpoons CO_{3,S}^{2-} \rightleftharpoons CO_2^g + e^- + O_S^- \tag{5c}$$

$$CO^S + 2O_S^- \rightleftharpoons CO_2^g + 2e^- + {}^1/_2O_S^- + S \tag{5d}$$

where the indices g and S refer to the gas phase and surface and O_S^- is taken as the dominant oxygen ionosorbed species at this temperature range.[39,40] It is also assumed that reactions proceed via the Langmuir−Hinshelwood mechanism with adsorbed CO (CO^S) as a precursor. If these reactions (eq 5) were the only processes governing the interaction between tin oxide and CO, then one would expect to observe a conductance recovery that would be proportional to the (ionosorbed) oxygen coverage, which would track the gate-potential dependence of the ionosorbed oxygen coverage. However, the observed dependence of ΔG_{CO} on gate potential is more complex (Figure 3, parts a and b). An important and reproducible feature of these data is the appreciable nonzero signal accompanying CO exposure, even at very negative gate potential values when the oxygen ionosorption was reduced essentially to zero. In a separate set of experiments, in which CO was admitted into the nitrogen flow (at zero gate potential) in the absence of oxygen, we determined that the adsorption of CO produces an increase in the source−drain current on its own. This phenomenon was also reported for the pristine thick SnO_2 films and those doped with metal promoters.[39,41]

This complex behavior can be reconciled if one assumes that there are at least two CO reaction channels. The second channel could be due to one (or more) of several processes such as reduction of lattice oxygens O_L^{2-} by CO

$$O_L^{2-} + CO^S \rightarrow CO_2^g + V_0 \quad V_0 \xrightarrow{kT} V_0^{\gamma+} + \gamma e^- \quad \gamma = 1, 2 \tag{6}$$

in contrast with the reactions (eq 5) between CO and ionosorbed oxygens (O_S^-).[41,42] Additionally, recent in situ combined conductometric, work function, and diffuse reflectance infrared Fourier transform (DRIFT) studies suggest that water impurities from the gas phase or surface hydroxyls preexisting on the surface strongly impede the sensing performance toward CO of nanostructured SnO_2 films.[43,44] Specifically, it was shown that under experimental conditions similar to ours CO interacts with surface hydroxyl groups (Sn^+ OH^-) creating an easily ionizable donor state (HO_L)[43,44]

$$CO + (Sn^+ OH^-) + O_L \rightarrow CO_2^g + Sn_L + (HO_L)^+ + e^- \tag{7}$$

Finally, CO itself was recently proposed to be a donor when adsorbed on tin oxide[39]

$$CO^g + S \rightleftharpoons CO_S \rightleftharpoons CO_S^+ + e^- \tag{8}$$

perhaps by creating a CO-derived intermediate on the surface acting as a Lewis base. Whichever of mechanisms (eqs 6−8) is active, the cumulative result is to create a reaction channel that does not involve ionosorbed oxygen that nevertheless increases the nanowire's conductance upon CO exposure.

When a mixture of CO and oxygen are simultaneously fed into the chamber, the response of the conductance will be affected by all of the processes (eqs 5−8), which proceed with electron exchange with the nanowire. However, the first reaction (eq 5) differs from the set of reactions (eqs 6−8) that we have lumped together as "the second channel". Specifically, the first reaction (eq 5) requires free electrons to be available near the nanowire surface for oxygen chemisorption to occur. The equilibrium density of free electrons is determined by the position of the Fermi level in the band gap, which in turn is controlled by the gate potential. Thus, the yield of the first reaction (eq 5) depends directly on the gate potential. By contrast, the second channel processes (eqs 6−8) contribute

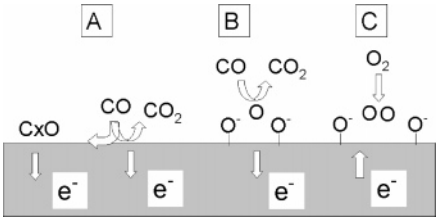

Figure 4. Schematic representation of the major donor−acceptor reaction channels assumed in our discussion: (A) putative CO adsorption processes denoted as C × O, which proceeds via reaction of CO with lattice oxygens, hydroxyl groups, etc. and has weak dependence (if any) on gate potential (for details see text); (B) reaction of CO with ionosorbed oxygens; (C) oxygen ionosorption (the desorption process not shown here). For representational simplicity, we only show the species O_S^-, which is likely the dominant chemisorbed species at this temperature.

electrons that will, in general, not have equilibrated with the lattice and hence will be less dependent on the gate potential. We therefore combine all of these possibilities into three phenomenological processes: (A) the reaction of the CO molecule with lattice oxygens (or with any of the other species discussed above) in which the "transient" electrons involved flow into the leads and only partially (if at all) participate in surface processes, (B) the reaction of CO with ionosorbed oxygen, whose equilibrium surface concentration depends on the availability of free electrons and therefore on the gate voltage, and (C) the ionosorption process itself, which is also affected by the gate potential. We also assume that CO and ionosorbed oxygens compete for adsorption sites on pristine nanowire. At constant gate potential, temperature, and gas concentration, these three processes will determine the steady-state coverage $\theta(V_{GS})$ of the ionosorbed oxygen, whose effect on conductance can be approximately described by the following equations that refer, respectively, to processes occurring under an O_2 in N_2 atmosphere and in a mixture of CO + O_2 + N_2.

$$G_1(V_{GS}) = \xi n(V_{GS}) - C\theta_1(V_{GS}) \tag{9a}$$

$$G_2(V_{GS}) = \xi n(V_{GS}) + A(1 - \theta_2(V_{GS})) + B\theta_2(V_{GS}) - C\theta_2(V_{GS}) \tag{9b}$$

The first term in both equations is the conductance $\pi R^2 e\mu n_0/L$ of the nanowire in dry nitrogen and *A*, *B*, and *C* are proportionality constants that reflect the efficiency of electron donation or withdrawal as shown schematically in Figure 4.

To simplify matters, we assume that $A \approx B$; that is, that the charge donated to the nanowire in the reaction of CO with lattice oxygens and with ionosorbed oxygens is nearly equivalent. Making this approximation and subtracting eq 9a from eq 9b, one gets

$$\Delta G_{CO}(V_{GS}) \approx A - C(\theta_2(V_{GS}) - \theta_1(V_{GS})) \tag{10}$$

which can be understood in terms of the experimental values plotted in Figure 3b. Equation 10 implies that there exists a gate-independent term (*A*) and a gate-dependent term proportional to the difference in the *steady-state* oxygen coverage that results from the addition of CO to the flowing O_2 + N_2 mixture. The quantity

$$\Delta G_{O_2}(V_{GS}) = C(\theta_1(V_{GS})) \tag{11}$$

is experimentally determinable. By combining the experimentally measured function $\Delta G_{O_2}(V_{GS})$ with eq 10, one can deduce the change in the (gate-dependent) steady-state coverage of

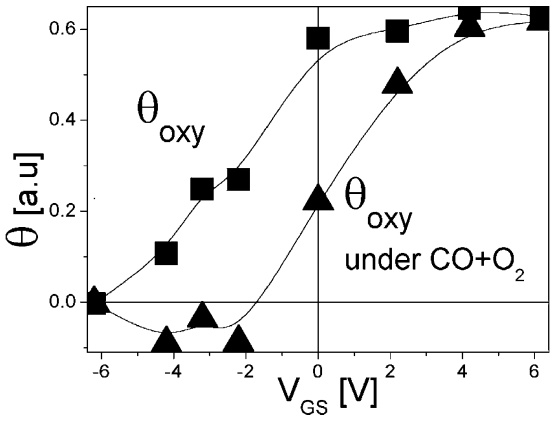

Figure 5. The relative steady-state ionosorbed oxygen coverage calculated from the observed conductance changes as a function of gate potential before (squares) and after (triangles) CO gas is admitted.

ionosorbed oxygen on admitting CO to the $N_2 + O_2$ gaseous stream. The result of such an analysis is shown in Figure 5, which plots the ionosorbed oxygen coverage as a function of the gate potential before and after CO is admitted into the flowing $N_2 + O_2$ mixture. The most notable effect of CO reacting with the surface oxygens is to shift the steady-state ionosorbed oxygen coverage to lower values at any given value of V_{GS} below approximately 4 V. At the most negative values of V_{GS}, the combined effect of the low electron density and the surface reactivity of CO is to essentially eliminate ionosorbed oxygen from the surface of the nanowire (triangles in Figure 5). Contrariwise, when electrons (and therefore ionosorbed oxygen) become plentiful (at positive values of V_{GS}, the impact of CO reactivity decreases, eventually to the point where its effect on the steady-state ionosorbed oxygen coverage becomes negligible even with CO present. This immediately explains the amonotonic evolution of $\Delta G_{CO}(V_{GS})$ in Figure 3b. At negative values of V_{GS} well below a threshold value, V_{th}, the conductance increase is almost solely determined by the reaction of CO with lattice oxygens. As the gate potential is increased, more ionosorbed oxygens survive exposure to CO, and $\Delta G_{CO}(V_{GS})$ reaches a maximum, then decreases again at a high enough, positive value of V_{GS}. At this point, the steady-state ionosorbed oxygen coverage with or without CO present in the gas flow is almost equal.

This behavior can be accounted for by assuming that both CO and oxygen compete for the same sites on the nanowire's surface. At negative values of V_{GS}, few oxygens adsorb because few electrons are available, leaving lots of room for CO to adsorb. However, these COs have few (ionosorbed oxygen) reaction partners on the surface with which to react, and CO reacts almost exclusively through channel A. As the gate potential is increased, more oxygen molecules ionosorb on the surface providing an increasing number of reaction partners for the coadsorbed COs. With a further increase in gate potential, more ionosorbed oxygens accumulate on the surface, eventually reducing the number of sites available for CO coadsorption, at which point CO reactivity (through channel B) reaches a maximum. With a further increase in gate potential, the extent of CO reactivity begins to decline as a result of the shortage of adsorbed CO molecules. Precisely that behavior was experimentally observed in ref 39 where it was shown that extended coadsorption of oxygen at SnO_2 film drastically reduces the sensitivity of the sensor toward CO. All the while, reaction through channel A takes place in a V_{GS}-independent (or weakly gate-dependent) process (Figure 3b).

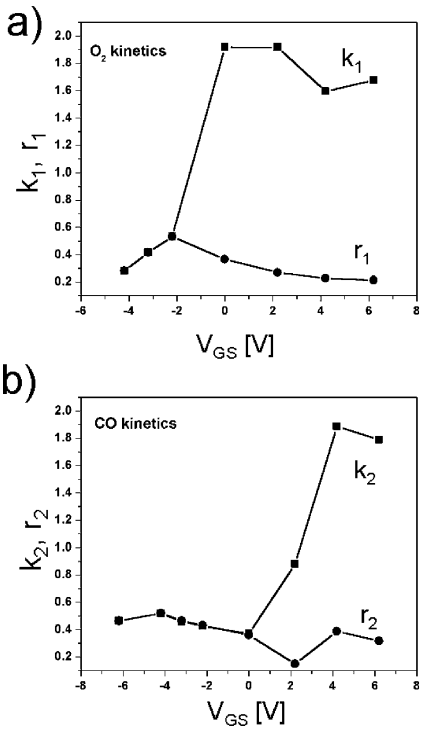

Figure 6. Rate constants (min^{-1}) obtained by fitting the time evolution of the conductance observed on (a) admitting oxygen and (b) admitting oxygen + CO entrained in nitrogen into the cell (Figure 3a) to sums of two exponentials (Supporting Information).

The above conclusions are supported by the results of a kinetic analysis that was carried out on the time evolution of the source−drain current, I_{SD}, shown in Figure 3a at various values of the gate potential. I_{SD} is assumed to reflect the electron density in the nanowire and hence the surface coverage by ionosorbed oxygen. The analyses were carried out independently on the decreasing and increasing portions of the current evolution with time following, respectively, the addition of oxygen, then $O_2 + CO$, to the flowing nitrogen (Figure 3a). The gate-voltage dependence of the rate constants determined in these analyses are given in Figure 6, parts a and b. Briefly, we found, for both the surface reactions with O_2 and with $O_2 + CO$, that at the most negative values of the gate potential the time evolution of I_{SD} was adequately reproduced by a single exponential (i.e., a single rate constant, $r_{1,2}$). Beyond a certain value of the gate potential, the time evolution of I_{SD} could no longer be fitted with a single exponential; however a sum of two exponentials (from which two rate constants, $r_{1,2}$ and $k_{1,2}$, were obtained) yielded a very good fit. Remarkably, one of the rate constants ($r_{1,2}$) was essentially independent of gate potential over the entire range of gate voltages used, while the second rate constant ($k_{1,2}$, which appeared only beyond a certain threshold value of the gate potential) showed a marked dependence on gate potential. (An analysis to show that the biexponential form is not an artifact of the finite time the pressure pulse of an added gas reaches its steady-state value is given in the Supporting Information.) Moreover, the threshold value (i.e., the value of V_{GS} at which biexponential behavior kicks in) occurs at a value approximately 2 V higher for the CO oxidation reaction (Figure 6b) as compared to the oxygen ionosorption reaction kinetics (Figure 6a). This shift mirrors almost exactly the shift in gate potential required to superimpose the ionosorbed oxygen coverage vs gate potential deduced from the analysis that led to Figure 5. The self-consistency of the

entire picture implies that, despite the many simplifications assumed, the basic mechanistic picture proposed is likely robust.

The above two-channel model of CO oxidation has an interesting implication for the use of nanowires as catalysts or sensors. In essence, we have shown that one can dramatically alter the branching ratio of the nanowire's catalytic action in the CO oxidation reaction simply by changing the gate potential under unchanging conditions of temperature, reactant composition, and pressure. Or when used as a sensor, this result suggests that the sensor's sensitivity to a given analyte could also be tuned, acting somewhat like an "electronic functionalization" of the nanowire's surface rendering it more or less sensitive to a given molecule (hence selective) by tuning the gate potential.

One can likewise foresee using this effect to observe and control catalytic activity on traditional (as well as novel) supported metal particles. Many metals traditionally used in catalysis (such as Pt or Pd) would form Schottky junctions with the semiconducting oxide of the nanowire. By use of a sufficiently small nanowire diameter, the depletion region of the Schottky junction would constrict the conductance channel through the nanowire to almost zero conductance. The size of this conductance channel could be further tailored using the gate potential. Moreover, if the metal particle is small enough, then it would contain sufficiently few electrons so that the electron exchange with the metal particle taking place as a result of surface chemistry at the metal surface would modulate the Schottky barrier strongly affecting the size of the conduction channel. Catalytic processes taking place on the surface of the metal nanoparticle would then be reflected in the source−drain current, in principle, even for a single metal particle, provided that its size, the nanowire's diameter, and the gate potential are chosen prudently. This would constitute a novel way for following catalytic processes occurring at supported metal catalyst particles. By controlling the gate potential, one could possibly also manipulate to some extent the catalytic reaction occurring on the metal particle's surface.

In summary, the electron-transport properties of individual tin oxide nanowires configured as FETs were determined over a wide temperature range in various atmospheres comprised of mixtures of $N_2/O_2/CO$. Because of their large surface-to-volume ratios, the bulk electronic properties of the nanowires were found to be controlled almost entirely by the chemical processes taking place at their surface, which could in turn be modified by controlling the gate potential. Thus, the rate and extent of oxygen ionosorption and the resulting rate and extent of catalytic CO oxidation reaction on the nanowire's surface could be controlled and even entirely halted by applying a negative enough gate potential. When optimized, such a single nanowire device could, in principle, be used as a tunable catalytic nanoreactor or a gas sensor with gate-selectable characteristics whose range and scope could be further expanded by appropriately functionalizing the surface.

Acknowledgment. We thank Professor Horia Metiu and Dr. Steeve Chretien for many insightful discussions. This work made extensive use of the MRL Central Facilities at UCSB supported by the National Science Foundation under MRSEC award No. DMR-0080034 and AFOSR DURINT Grant F49620-01-1-0459.

Supporting Information Available: Analysis showing that the biexponential form is not an artifact of the finite time the pressure pulse of an added gas reaches its steady-state value.This material is available free of charge via the Internet at http://pubs.acs.org.

References and Notes

(1) Huang, M. H.; Mao, S.; Feick, H.; Yan, H. Q.; Wu, Y. Y.; Kind, H.; Weber, E.; Russo, R.; Yang, P. D. *Science* **2001**, *292*, 1897.
(2) Pan, Z. W.; Dai, Z. R.; Wang, Z. L. *Science* **2001**, *291*, 1947.
(3) Comini, E.; Faglia, G.; Sberveglieri, G.; Pan, Z. W.; Wang, Z. L. *Appl. Phys. Lett.* **2002**, *81*, 1869.
(4) Arnold, M. S.; Avouris, P.; Pan, Z. W.; Wang, Z. L. *J. Phys. Chem. B* **2003**, *107*, 659.
(5) Wu, Y. Y.; Yan, H. Q.; Yang, P. D. *Top. Catal.* **2002**, *19*, 197.
(6) Li, C.; Zhang, D. H.; Han, S.; Liu, X. L.; Tang, T.; Zhou, C. W. *Adv. Mater.* **2003**, *15*, 143.
(7) Collins, P. G.; Bradley, K.; Ishigami, M.; Zettl, A. *Science* **2000**, *287*, 1801.
(8) Kong, J.; Franklin, N. R.; Zhou, C. W.; Chapline, M. G.; Peng, S.; Cho, K. J.; Dai, H. J. *Science* **2000**, *287*, 622.
(9) Kong, J.; Chapline, M. G.; Dai, H. J. *Adv. Mater.* **2001**, *13*, 1384.
(10) Cui, Y.; Wei, Q. Q.; Park, H. K.; Lieber, C. M. *Science* **2001**, *293*, 1289.
(11) Law, M.; Kind, H.; Messer, B.; Kim, F.; Yang, P. D. *Angew. Chem., Int. Ed.* **2002**, *41*, 2405.
(12) Li, C.; Zhang, D. H.; Liu, X. L.; Han, S.; Tang, T.; Han, J.; Zhou, C. W. *Appl. Phys. Lett.* **2003**, *82*, 1613.
(13) Gopel, W. *Sens. Actuators* **1989**, *16*, 167.
(14) Sberveglieri, G. *Sens. Actuators, B* **1992**, *6*, 239.
(15) Yamazoe, N.; Miura, N. *Sens. Actuators, B* **1994**, *20*, 95.
(16) Moseley, P. T. *Meas. Sci. Technol.* **1997**, *8*, 223.
(17) Kohl, D. *J. Phys. D: Appl. Phys.* **2001**, *34*, R125.
(18) Zhang, Y.; Kolmakov, A.; Chretien, S.; Metiu, H.; Moskovits, M. *Nano Lett.* **2004**, *4*, 403.
(19) Hellmich, W.; Muller, G.; Bosch-Von Braunmuhl, C.; Doll, T.; Eisele, I. *Sens. Actuators, B* **1997**, *43*, 132.
(20) Scharnagl, K.; Bogner, M.; Fuchs, A.; Winter, R.; Doll, T.; Eisele, I. *Sens. Actuators, B* **1999**, *57*, 35.
(21) Lakshmi, B. B.; Dorhout, P. K.; Martin, C. R. *Chem. Mater.* **1997**, *9*, 857.
(22) Masuda, H. *Electrochemistry* **2001**, *69*, 879.
(23) Routkevitch, D.; Tager, A. A.; Haruyama, J.; Almawlawi, D.; Moskovits, M.; Xu, J. M. *IEEE Trans. Electron Devices* **1996**, *43*, 1646.
(24) Metzger, R. M.; Konovalov, V. V.; Sun, M.; Xu, T.; Zangari, G.; Xu, B.; Benakli, M.; Doyle, W. D. *IEEE Trans. Magn.* **2000**, *36*, 30.
(25) Nicewarner-Pena, S. R.; Freeman, R. G.; Reiss, B. D.; He, L.; Pena, D. J.; Walton, I. D.; Cromer, R.; Keating, C. D.; Natan, M. J. *Science* **2001**, *294*, 137.
(26) Kolmakov, A.; Zhang, Y.; Moskovits, M. *Nano Lett.* **2003**, *3*, 1125.
(27) Dai, Z. R.; Gole, J. L.; Stout, J. D.; Wang, Z. L. *J. Phys. Chem. B* **2002**, *106*, 1274.
(28) Kim, W.; Javey, A.; Vermesh, O.; Wang, O.; Li, Y. M.; Dai, H. J. *Nano Lett.* **2003**, *3*, 193.
(29) Barsan, N.; Weimar, U. *J. Electroceram.* **2001**, *7*, 143.
(30) Kolmakov, A.; Zhang, Y.; Cheng, G.; Moskovits, M. *Adv. Mater.* **2003**, *15*, 997.
(31) Schierbaum, K. D.; Weimar, U.; Gopel, W.; Kowalkowski, R. *Sens. Actuators, B* **1991**, *3*, 205.
(32) Barsan, N.; Schweizer-Berberich, M.; Gopel, W. *Fresenius' J. Anal. Chem.* **1999**, *365*, 287.
(33) Avouris, P.; Hertel, T.; Martel, R.; Schmidt, T.; Shea, H. R.; Walkup, R. E. *Appl. Surf. Sci.* **1999**, *141*, 201.
(34) Avouris, P.; Martel, R.; Derycke, V.; Appenzeller, J. *Physica B* **2002**, *323*, 6.
(35) Huang, Y.; Duan, X. F.; Wei, Q. Q.; Lieber, C. M. *Science* **2001**, *291*, 630.
(36) Huang, Y.; Duan, X. F.; Cui, Y.; Lauhon, L. J.; Kim, K. H.; Lieber, C. M. *Science* **2001**, *294*, 1313.
(37) Huang, Y.; Duan, X. F.; Cui, Y.; Lieber, C. M. *Nano Lett.* **2002**, *2*, 101.
(38) Martel, R.; Schmidt, T.; Shea, H. R.; Hertel, T.; Avouris, P. *Appl. Phys. Lett.* **1998**, *73*, 2447.
(39) Hahn, S. H.; Barsan, N.; Weimar, U.; Ejakov, S. G.; Visser, J. H.; Soltis, R. E. *Thin Solid Films* **2003**, *436*, 17.
(40) Sinner-Hettenbach, M.; Barsan, N.; Weimar, U.; Weiss, T.; von Schenck, H.; Gothelid, M.; Giovanelli, L.; Le Lay, G. *Thin Solid Films* **2001**, *391*, 192.
(41) Safonova O, B. I., Fabrichnyi P, Rumyantseva M, Gaskov A. *J. Mater. Chem.* **2002**, *12*, 11.
(42) Henrich, V. E.; Cox, P. A. *Surface Science of Metal Oxides*; Cambridge University Press: Cambridge, New York, 1996.
(43) Harbeck, S.; Szatvanyi, A.; Barsan, N.; Weimar, U.; Hoffmann, V. *Thin Solid Films* **2003**, *436*, 76.
(44) Barsan, N.; Weimar, U. *J. Phys.: Condens. Matter* **2003**, *15*, R813.